Proteogenomic profiling uncovers differential therapeutic vulnerabilities between *TCF3::PBX1* and *TCF3::HLF* translocated B-cell acute lymphoblastic leukemia

Although therapy escalation has led to improved 5-year overall survival rates for patients with B-cell acute lymphoblastic leukemia (B-ALL), few effective treatment options are available for relapsed and treatment-resistant disease. This applies particularly to specific subtypes of B-ALL, such as patients harboring *TCF3* (formerly *E2A*) fusions. *TCF3*, encoding members of the E protein (class I) family of helix-loop-helix transcription factors, is a master regulator of B-cell development and is involved in several chromosomal translocations associated with lymphoid malignancies, such as the translocation t(1;19)(q23;p13.3), resulting in the *TCF3::PBX1* fusion (5% of pediatric B-ALL) or the translocation t(17;19)(q22;p13) generating the *TCF3::HLF* fusion (~0.5% of pediatric B-ALL).[2] Omics research for the discovery of novel treatment strategies in hematological cancer is still based largely on transcriptomics, although it is increasingly recognized that this does not translate well into the expression of proteins, which are the main targets of drugs and functional entities of biological processes. In this study, we comprehensively analyzed the proteomic landscapes of *TCF3::HLF*$^+$ (N=6) and *TCF3::PBX1*$^+$ (N=5) B-ALL employing primary patient-derived xenografts (PDX), liquid chromatography tandem mass spectrometry and data-dependent acquisition. Approval for the study reported here was granted by the Ethics Committee of the Medical Faculty of the Christian-Albrechts-University, Kiel, Germany (vote D508/13). We detected 6,863 proteins (6,123 without ≥2 missing values; *Online Supplementary Table S1*), which allowed a clear distinction between *TCF3::HLF*$^+$ and *TCF3::PBX1*$^+$ leukemia by unsupervised hierarchical clustering and principal component analysis (Figure 1A, B). Proteomic profiling proved a useful tool for prioritizing drug targets, as only 8.45% of the significantly differentially expressed genes (N=119/1,409; P<0.05 and minimal $\log_2$ fold change of ±1) previously detected by RNA sequencing[2] showed differential expression on protein level confirmed by our proteomic analysis (*Online Supplemenary Figure S1A*). In contrast, 34.8% (N=119/342) of differentially regulated proteins detected by proteomics were also differentially expressed on RNA level. As a proof-of-concept, we examined overlap of differentially expressed genes (cutoffs: P<0.05 and minimal $\log_2$ fold change of ±1) from RNA sequencing and proteomic analysis obtained from a previously published dataset of *ETV6::RUNX1*$^+$ (N=9) and high hyperdiploid (N=18) primary ALL patient samples.[3] While only 3.63% (N=82/2,262) of differentially expressed genes detected via RNA sequencing showed differential expression on protein level, 92.13% (N=82/89) of differentially regulated proteins were also differentially expressed on RNA level (*Online Supplementary Figure S1B*).

In order to identify protein classes presenting specific therapeutic vulnerabilities, we performed gene set enrichment analysis (GSEA). We identified several gene sets enriched in either of the two subgroups (Figure 1C). RNA biology, mitochondrial translation and cellular respiration were the most prominent enriched gene sets for *TCF3::HLF*$^+$ leukemia. In addition, strongly increased MYC expression and enrichment in MYC targets (Figure 1D, E) were detected, consistent with TCF3::HLF-driven activation of a *MYC* enhancer cluster previously shown using extensive functional genomics.[4] For *TCF3::PBX1*$^+$ leukemia, immune response/cell cycle, actin cytoskeleton, cell morphogenesis and RTK signaling were among the most prominent enriched gene sets (Figure 1C). We validated therapeutic vulnerabilities indicated by GSEA using high-throughput drug screening. To this end, we tested the sensitivity of leukemic cell lines (*TCF3::HLF*$^+$: HAL-01; *TCF3::PBX1*$^+$: 697 and RCH-ACV) and mononuclear cells from peripheral blood of three healthy donors against a drug library of over 600 Food and Drug Administration-approved or clinical trial phase I-IV anti-cancer drugs. *TCF3::HLF*$^+$ and *TCF3::PBX1*$^+$ leukemic cells showed a differential response towards 109 drugs based on the area under the curve (AUC) as response parameter (Figure 2A; *Online Supplementary Table S2*; AUC<0.8 and >1.2 as a cutoff). Compared to our previous screening of bioactive compounds (N=98) employing the PDX samples,[2] the cell lines showed similarly increased sensitivity towards compounds, such as BCL2 and mTOR inhibitors for *TCF3::HLF*$^+$, and aurora kinase and polo-like kinase inhibitors for *TCF3::PBX1*$^+$ B-ALL (Figure 2A). In addition, we identified novel potential drug targets. These included MDM2 and DNA/RNA synthesis for *TCF3::HLF*$^+$ and microtubule/tubulin and cyclin-dependent kinases (CDK) for *TCF3::PBX1*$^+$ leukemic cells (Figure 2A). In order to confirm these findings, we chose drugs from those groups, which did not affect normal peripheral blood cells (Figure 2B-E), and treated *TCF3::PBX1*$^+$ (RCH-ACV) and *TCF3::HLF*$^+$ (HAL-01) cells with half half-maximal inhibitory concentration (IC_{50}), IC_{50} and double IC_{50} concentrations to investigate apoptosis induction. We demonstrated increased caspase 3/7 activity and apoptotic subG$_1$ cells in *TCF3::PBX1*$^+$ B-ALL in response to the microtubule/tubulin inhibitor ixabepilone and the CDK inhibitor SNS-032. For *TCF3::HLF*$^+$ leukemic cells, we verified increased apoptotic cell death upon idasanutlin

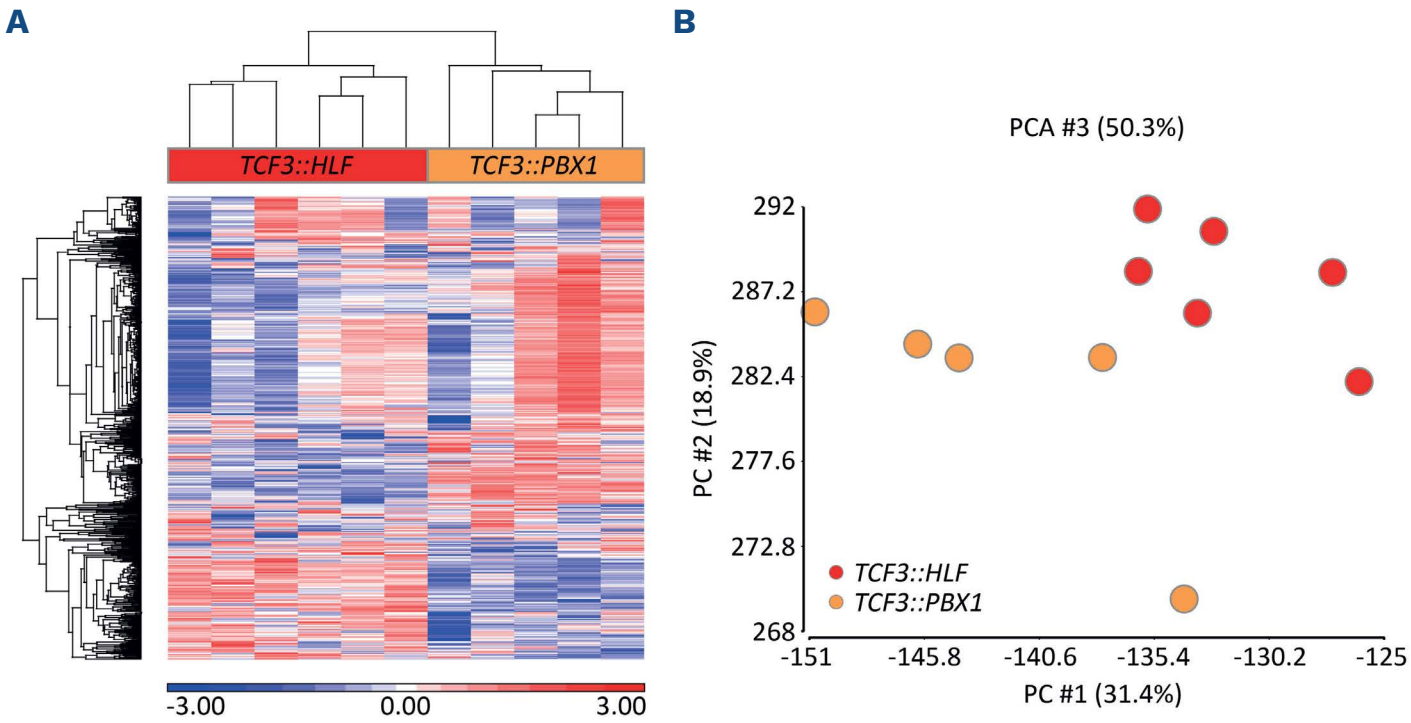

Figure 1. Proteomic profiling distinguishes *TCF3::HLF*⁺ and *TCF3::PBX1*⁺ leukemia and uncovers therapeutic vulnerabilities for both subtypes. Unsupervised hierarchical clustering (A), principal component analysis (PCA) (B) and gene set enrichment analysis (GSEA) (C) was performed on the proteomic data of 6 *TCF3::HLF*⁺ (in red) and 5 *TCF3::PBX1*⁺ (in orange) B-cell acute lymphoblastic leukemia (B-ALL) patient-derived xenograft samples. For unsupervised hierarchical clustering, the 10% most variable proteins were used based on the standard deviation. PCA was performed on all proteins. Both subtypes clearly segregate into distinct clusters suggesting highly distinct proteomic landscapes. (C) GSEA is based on all proteins and identifies several gene sets enriched in either of the two subgroups. (D) Proteomic data shows enrichment of MYC protein expression in *TCF3::HLF*⁺ *versus TCF3::PBX1*⁺ leukemic samples in this study. In order to determine differential expression, non-parametric Mann-Whitney *t* test (two-tailed) was used. (E) Gene set enrichment plot of MYC targets showing a positive correlation with *TCF3::HLF*⁺ leukemia.

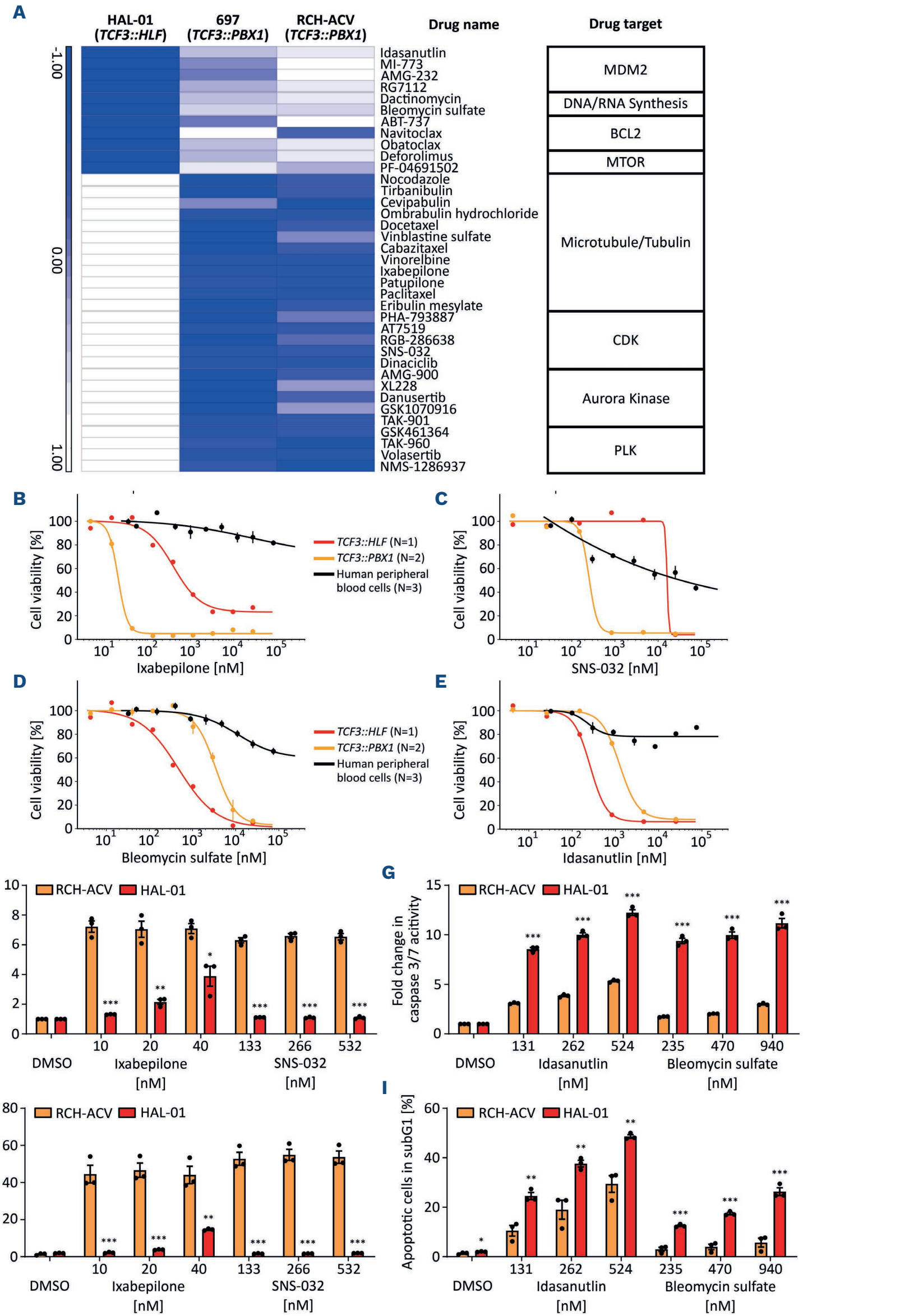

Continued on following page.

Figure 2. High-throughput drug screening and functional analysis confirm therapeutic vulnerabilities for *TCF3::HLF*⁺ and *TCF3::PBX1*⁺ leukemic cells. (A) HAL-01 (*TCF3::HLF*⁺), 697 and RCH-ACV (both *TCF3::PBX1*⁺) were exposed to a drug library, consisting of over 600 compounds. The supervised heatmap is based on the area under the curve (AUC, minimal fold change of <0.8 or >1.2 as a cutoff) as response parameter. Presented are groups of drugs with a differential response between *TCF3::PBX1*⁺ and *TCF3::HLF*⁺ leukemic cells. High sensitivity is shown in blue and low sensitivity is shown in white. (B-E) Presented are the dose-response curves for ixabepilone (B), SNS-032 (C), bleomycin sulfate (D) and idasanutlin (E), showing a differential response of *TCF3::HLF*⁺ *versus* *TCF3::PBX1*⁺ leukemic cells. Human peripheral blood cells from 3 healthy donors (in black) served as control cells (B-E). (F-I) RCH-ACV and HAL-01 were treated with ixabepilone (10 nM, 20 nM, 40 nM), SNS-032 (133 nM, 266 nM, 532 nM), idasanutlin (131 nM, 262 nM, 524 nM) or bleomycin sulfate (235 nM, 470 nM, 940 nM) dissolved in dimethyl sulfoxide (DMSO) or DMSO as negative control. (F, G) Bar graphs representing the fold change in caspase 3/7 activity 24 hours after treatment. Caspase 3/7 activity was determined using the Caspase-Glo 3/7 Assay (Promega). (H, I) Bar graphs represent the proportion of apoptotic cells (subG$_1$) 48 hours after treatment. Cell cycle profiles were generated by flow cytometric measurement of propidium iodide intercalation into DNA after partial cell lysis in hypotonic buffer (0.1% sodium citrate, 0.1% Triton X-100, 0.5 mg/mL RNase A containing 40 µg/mL propidium iodide). Values shown in (F-I) represent mean ± standard error of the mean of 3 biologically independent replicates. NS: not significant; *P<0.05; **P<0.01; ***P<0.001 (*t* test).

(MDM2 inhibitor) and bleomycin sulfate (DNA/RNA synthesis inhibitor) treatment (Figure 2F-I).

Besides the detection of vulnerabilities to specific drug classes, we aimed to identify novel targets for drug development. In our proteomic analyses, the B-lymphoid tyrosine kinase (BLK) was the most significantly upregulated protein for the *TCF3::PBX1*⁺ subtype (Figure 3A; *Online Supplementary Figure S1C; Online Supplementary Table S1;* minimal $\log_2$ fold change of ±1 and significance level of P<0.05 as cutoffs). *BLK* encodes a non-receptor tyrosine kinase of the src family of proto-oncogenes that plays an important role in precursor (pre) B-cell receptor (BCR) signaling and early B-cell development.[5] RNA-sequencing and expression microarray data by us and others supported this finding (Figure 3B-D). We examined human gene expression data derived from four independent data sets of >3,000 leukemia cases[6-9] available at the R2: genomics analysis and visualization platform (http://r2.amc.nl). These data indicated a subpopulation of leukemia samples that highly co-expresses *BLK* and *PBX1* (Figure 3B; *Online Supplementary Figure S1D-F*). In two of the data sets, information on chromosomal translocations was available. There, the *BLK* and *PBX1* co-expressing subpopulation was specifically associated with the *TCF3::PBX1* fusion (Figure 3B; *Online Supplementary Figure S1D*).[8,9] In the Microarray Innovations in LEukemia (MILE) study[8] all 36 cytogenetically identified *TCF3::PBX1*⁺ cases were *BLK*^{high} expressing (N=1,897 other leukemia or myelodysplastic syndrome [MDS], N=71 normal controls). Similarly, in another study[9] all six *TCF3::PBX1*⁺ cases and none of the other samples (N=185 other B-ALL, N=3 normal controls) were both *PBX1* and *BLK* high expressing. RNA-sequencing data of our cohort showed high RNA expression of *BLK* in all *TCF3::PBX1*⁺ leukemia cases (N=5 at diagnosis, N=8 after transplantation into NSG mice)[2] compared to *TCF3::HLF*⁺ cases (N=5 at diagnosis, N=22 after transplantation) (Figure 3C, D).

Thus, we hypothesized that interference with BLK signaling might present a potential treatment strategy for *TCF3::PBX1*-rearranged B-ALL in particular. In order to test this, we treated *TCF3::PBX1*⁺ BLK^{high} (RCH-ACV) and *TCF3::HLF*⁺ BLK^{low} (HAL-01) cells with a first selective irreversible BLK inhibitor BLK-IN-2.[10] BLK^{high} cells responded in a dose-dependent manner starting at nanomolar concentrations (IC_{50}=0.2169 µM), whereas BLK^{low} cells showed little or no response (≥167-fold less, IC_{50}=36.20 µM) (Figure 3E; *Online Supplementary Figure S1G-I*). We further tested the impact of BLK-IN-2 on other genetic subtypes of B-ALL and noticed preferential sensitivity of only the *TCF3::PBX1*⁺ subtype to BLK-IN-2 (*Online Supplementary Figure S1I*). In order to test if BLK inhibition synergizes with the specific vulnerabilities identified in our proteomic screen, we performed combined treatment with ixabepilone (microtubule/tubulin inhibitor). Indeed, both drugs synergized in *TCF3::PBX1*⁺ cell lines, but not in the *TCF3::HLF*⁺ cell line HAL-01 (Figure 3F-H). We further tested, if interference with pre-BCR signaling including BTK inhibitors would have the same impact. To this end, we tested the response of *TCF3::PBX1*⁺ B-ALL cell lines to ibrutinib and other BTK-targeting drugs (acalabrutinib, spebrutinib, LFM-A13). The response, however, was low and did not differ from cells lacking pre-BCR expression.

As previously reported by Geng *et al.*, *BLK* is a signature gene of adult *TCF3::PBX1*⁺ B-ALL.[9] Combining chromatin immoprecipitation sequencing, DNA methylation and expression profiling, the authors identified hypomethylation and overexpression of *BLK* in adult *TCF3::PBX1*⁺ B-ALL. In this study, upregulated genes targeted by TCF3::PBX1 included pre-BCR components and pre-BCR downstream signaling molecules.[11] Ligand-independent autonomous tonic pre-BCR activation via self-aggregation is a main mechanism for pre-BCR activation and leads to constitutive activation of BLK[11] (indicated by phosphorylation of the activating tyrosine Y388) observed in several *TCF3::PBX1*⁺ cell lines and primary B-ALL.[11] Pre-BCR function induces activation of the transcription factor *BCL6*, which further increases pre-BCR signaling in a self-enforcing positive feedback loop and directly activates *BLK* transcription. More than 90% of *TCF3::PBX1*⁺ leukemia cases are pre-BCR⁺ and critically rely on pre-BCR-dependent signaling for proliferation.[5] Thus, targeting BLK to abrogate pre-BCR downstream signaling presents an attractive approach for therapeutic intervention in *TCF3::PBX1*⁺ B-ALL.

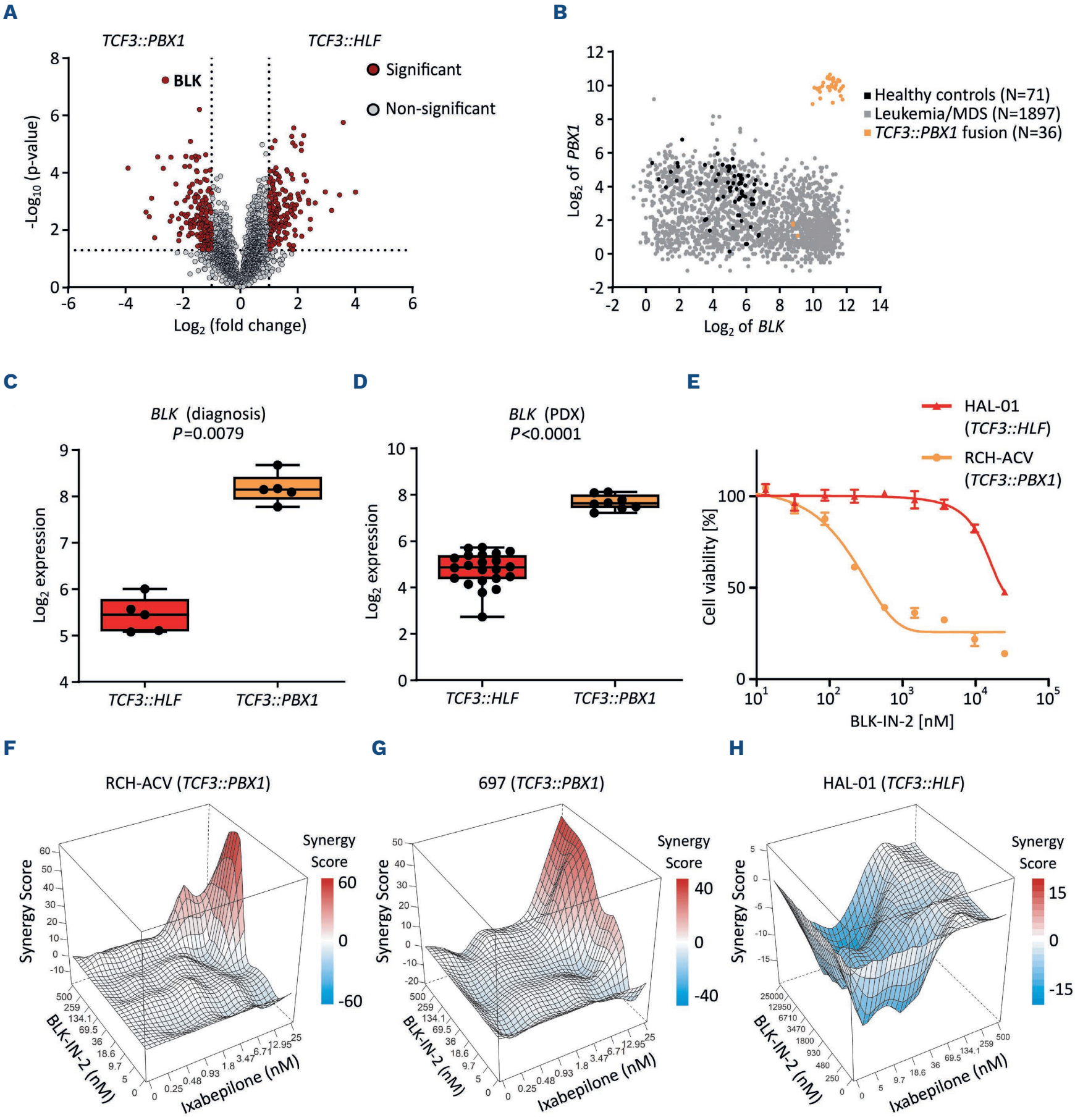

Figure 3. Proteogenomic profiling detects BLK as a marker of *TCF3::PBX1*⁺ B-cell acute lymphoblastic leukemia targetable by the selective BLK inhibitor BLK-IN-2. (A) The volcano plot presents significantly (red) or non-significantly (grey) dysregulated proteins in *TCF3::PBX1*⁺ (left) or *TCF3::HLF*⁺ (right) leukemias. BLK is the most significantly dysregulated protein for the *TCF3::PBX1*⁺ subtype (minimal $\log_2$ fold change of ±1 and significance level of $P<0.05$ as cutoffs). (B) Gene expression data of human patient samples is derived from data sets available at the R2: genomics analysis and visualization platform (http://r2.amc.nl). Dot plot presents *PBX1* and *BLK* expression in healthy controls (black), *TCF3::PBX1*⁺ (orange) and other unstratified leukemic samples (grey). Data of the Mixed Leukemia - MILE - 2004 - MAS5.0 - u133p2 study[8] is shown. Three further studies are presented in the *Online Supplementary Figure S1D-F*. (C,D) *BLK* RNA expression in *TCF3::HLF*⁺ (N=5) and *TCF3::PBX1*⁺ (N=5) B-ALL at the time of diagnosis (C) and after transplantation into NSG mice (*TCF3::HLF*⁺: N=22; *TCF3::PBX1*⁺: N=8). (D). Data is derived from our previous study.[2] In order to determine differential expression, non-parametric Mann-Whitney *t* test (two-tailed) was used. (E) Dose-response curves for BLK-IN-2 show a differential response of *TCF3::HLF*⁺ (red) *versus* *TCF3::PBX1*⁺ (orange) leukemic cells. (F-H) Synergy drug screening of BLK-IN-2 and Ixabepilone reveals a strong synergistic effect in *TCF3::PBX1*⁺ cell lines, while no such effect is detected in the *TCF3::HLF*⁺ cell line HAL-01. Representative synergy plots of 3 independent experiments are shown. Drug concentration ranges were chosen according to the predetermined half-maximal inhibitory concentration (IC_{50}) values of each cell line (RCH-ACV. and 697: 5-500 nM BLK-IN-2, 0.25-25 nM ixabepilone; HAL-01: 0.25-25 μM BLK-IN-2, 5-500 nM ixabepilone). Dimethyl sulfoxide (DMSO) was used as a negative control. ZIP synergy score analysis was conducted using the synergyfinder package version 3.0.14 with additional baseline correction.

Previously, interference with pre-BCR signaling has been suggested as a therapeutic option for *TCF3*-rearranged ALL[12] and the inhibitors ibrutinib, dasatinib and idelalisib to be effective against *TCF3::PBX1*$^+$ B-ALL.[5,12,13] Inhibition of BTK, a downstream signaling kinase of the BCR, by ibrutinib is clinically beneficial in BCR$^+$ B-cell malignancies such as non-Hodgkin lymphomas and multiple myeloma. However, in our analyses, the response of *TCF3::PBX1*$^+$ B-ALL cell lines to BTK-targeting drugs was low and not corresponding to pre-BCR expression. This is in line with the observation that ibrutinib exerts a cytostatic rather than a cytotoxic effect on pre-BCR$^+$ B-ALL cells[5] and is further supported by the lack of *in vivo* effectivity against *TCF3::PBX1*$^+$ primogafts.[14] However, *TCF3::PBX1*$^+$ PDX samples responded well to the tyrosine kinase inhibitor dasatinib.[2] Still, high doses might be required for targets other than *BCR::ABL1* and might be limited in the relapse setting due to toxicity.[13]

Taken together, proteomic-based profiling is a powerful tool to discover highly specific and sensitive cancer biomarkers and oncogenic pathway activation.[15] Here, we uncovered proteomic alterations associated with *TCF3::HLF*$^+$ or *TCF3::PBX1*$^+$ B-ALL and revealed potential therapeutic options for these subtypes. These include previously known sensitivities for *TCF3::HLF*$^+$ (e.g., BCL2 and mTOR) and *TCF3::PBX1*$^+$ B-ALL (e.g., aurora kinase and polo-like kinase), as well as potential novel drug targets, such as MDM2 and DNA/RNA synthesis for *TCF3::HLF*$^+$ or microtubule/tubulin and CDK for *TCF3::PBX1*$^+$ leukemic cells. Our data suggest that *TCF3::PBX1*$^+$ B-ALL might be sensitive to treatment with selective BLK inhibitors, especially in combination with microtubule/tubulin targeting drugs, such as ixabepilone. Due to high BLK expression in *TCF3::PBX1*$^+$ B-ALL cells, such inhibitors could selectively eradicate leukemic cells at doses eliciting less side-effects on normal tissue. A limitation of our study is that this was not tested in mouse models. In future studies, it would be interesting to apply BLK inhibition to suitable mouse models of *TCF3::PBX1*$^+$ leukemia and to test synergism with other drugs. Larger numbers of patient samples need to be tested to show the applicability for *TCF3::PBX1*$^+$ leukemia.

Authors

Lena Blümel,[1,2] Flavia Bernardi,[3,4] Daniel Picard,[1,2] Jacob Torrejon Diaz,[3,4] Vera H. Jepsen,[1,5] Rebecca Hasselmann,[1,5] Julian Schliehe-Diecks,[1,5] Jasmin Bartl,[1,2,6] Nan Qin,[1,2] Beat Bornhauser,[7] Sanil Bhatia,[1,5] Blerim Marovka,[7] Veronique Marsaud,[3,4] Florent Dingli,[8] Damarys Loew,[8] Martin Stanulla,[9#] Jean-Pierre Bourqin,[7#] Arndt Borkhardt,[1,5#] Marc Remke,[1,2#] Olivier Ayrault[3,4#] and Ute Fischer[1,5#]

[1]Department of Pediatric Oncology, Hematology and Clinical Immunology, Heinrich Heine University Düsseldorf, Medical Faculty, and University Hospital Düsseldorf, Düsseldorf, Germany; [2]Division of Pediatric Neuro-Oncogenomics, German Cancer Research Center (DKFZ) and German Cancer Consortium (DKTK), partner site Essen/Düsseldorf, Düsseldorf, Germany; [3]Institut Curie, CNRS UMR, INSERM, PSL Research University, Orsay, France; [4]CNRS UMR 3347, INSERM U1021, Université Paris Sud, Université Paris-Saclay, Orsay, France; [5]German Cancer Consortium (DKTK), partner site Essen/Düsseldorf, Düsseldorf, Germany; [6]Group for Interdisciplinary Neurobiology and Immunology - INI-research, Institute of Zoology, University of Hamburg, Hamburg, Germany; [7]Department of Oncology and Children's Research Center, University Children's Hospital Zurich, Zurich, Switzerland; [8]Institut Curie, PSL Research University, Centre de Recherche, CurieCoreTech Spectrométrie de Masse Protéomique, Paris, France and [9]Department of Pediatric Hematology and Oncology, Hannover Medical School, Hannover, Germany

[#]MS, J-PB, AB, MR, OA and UF contributed equally as senior authors.

Correspondence:
U. FISCHER - ute.fischer@med.uni-duesseldorf.de

https://doi.org/10.3324/haematol.2023.283928

Received: July 17, 2023.
Accepted: February 15, 2024.
Early view: February 29, 2024.

Disclosures

No conflicts of interest to disclose.

Contributions

LB, JB, MS, J-PB, AB, MR, OA and UF planned and directed the study. Patient-derived xenograft models were provided by BB, BM and J-PB. FB, JTD, VM, FD, DL and OA conducted proteomic profiling and analyzed proteomic data. DP provided bioinformatic analyses. LB designed and performed the in vitro experiments, supported by VJ, JS-D and RH. NQ generated dose-response curves. SB provided intellectual contributions to the project and to the interpretation of the results. LB, VJ and UF wrote the manuscript. Figures were designed and drafted by LB, DP, NQ, VJ, JS-D and UF. All authors edited and contributed to the final manuscript.

Acknowledgments

Frauke-Dorothee Meyer, Sarah Göbbels and Bianca Killing are acknowledged for excellent technical assistance.

Funding

This work was supported by grants from the German José-Carreras Leukemia Foundation (DJCLS 07 R/2019 [to AB], DJCLS 18R/2021 [to UF], DJCLS 21R/2019 [to MR and UF]), the Elterninitiative Kinderkrebsklinik e.V. (to MR and JB), the Katharina-Hardt-Stiftung (to AB), the parents' initiative Löwenstern e.V. (to AB and UF), the Gert-und-Susanna-Meyer Foundation (to MR), the Research Commission of the Medical Faculty of the Heinrich Heine University (to MR and NQ), the German Research Foundation (HE 8807/3-1 [to

UF], RE 2857/2-1 and KFO 337 [to MR]), the German Cancer Aid (Deutsche Krebshilfe, grant no. 111537 [to MR]) and the "Cancer Prevention - Graduate School" by German Cancer Aid, grant no. 70114736 and coordinated by the German Cancer Research Center (DKHZ), grant no. 70114766 (to UF), and the Saint Baldrick's Robert J. Arceci Innovation Award (to OA).

Data-sharing statement

The data set generated and analyzed during the current study will be made available at PRIDE.[1]

References

1. Perez-Riverol Y, Bai J, Bandla C, et al. The PRIDE database resources in 2022: a hub for mass spectrometry-based proteomics evidences. Nucleic Acids Res. 2022;50(D1):D543-D552.
2. Fischer U, Forster M, Rinaldi A, et al. Genomics and drug profiling of fatal TCF3-HLF-positive acute lymphoblastic leukemia identifies recurrent mutation patterns and therapeutic options. Nat Genet. 2015;47(9):1020-1029.
3. Yang M, Vesterlund M, Siavelis I, et al. Proteogenomics and Hi-C reveal transcriptional dysregulation in high hyperdiploid childhood acute lymphoblastic leukemia. Nat Commun. 2019;10(1):1519.
4. Huang Y, Mouttet B, Warnatz HJ, et al. The Leukemogenic TCF3-HLF complex rewires enhancers driving cellular identity and self-renewal conferring EP300 vulnerability. Cancer Cell. 2019;36(6):630-644.
5. Kim E, Hurtz C, Koehrer S, et al. Ibrutinib inhibits pre-BCR(+) B-cell acute lymphoblastic leukemia progression by targeting BTK and BLK. Blood. 2017;129(9):1155-1165.
6. Polak R, Bierings MB, van der Leije CS, et al. Autophagy inhibition as a potential future targeted therapy for ETV6-RUNX1-driven B-cell precursor acute lymphoblastic leukemia. Haematologica. 2019;104(4):738-748.
7. Loh ML, Zhang J, Harvey RC, et al. Tyrosine kinome sequencing of pediatric acute lymphoblastic leukemia: a report from the Children's Oncology Group TARGET Project. Blood. 2013;121(3):485-488.
8. Kohlmann A, Kipps TJ, Rassenti LZ, et al. An international standardization programme towards the application of gene expression profiling in routine leukaemia diagnostics: the Microarray Innovations in LEukemia study prephase. Br J Haematol. 2008;142(5):802-807.
9. Geng H, Brennan S, Milne TA, et al. Integrative epigenomic analysis identifies biomarkers and therapeutic targets in adult B-acute lymphoblastic leukemia. Cancer Discov. 2012;2(11):1004-1023.
10. Fu T, Zuo Y, Zhong Z, Chen X, Pan Z. Discovery of selective irreversible inhibitors of B-Lymphoid tyrosine kinase (BLK). Eur J Med Chem. 2022;229:114051.
11. Geng H, Hurtz C, Lenz KB, et al. Self-enforcing feedback activation between BCL6 and pre-B cell receptor signaling defines a distinct subtype of acute lymphoblastic leukemia. Cancer Cell. 2015;27(3):409-425.
12. van der Veer A, van der Velden VH, Willemse ME, et al. Interference with pre-B-cell receptor signaling offers a therapeutic option for TCF3-rearranged childhood acute lymphoblastic leukemia. Blood Cancer J. 2014;4(2):e181.
13. Eldfors S, Kuusanmaki H, Kontro M, et al. Idelalisib sensitivity and mechanisms of disease progression in relapsed TCF3-PBX1 acute lymphoblastic leukemia. Leukemia. 2017;31(1):51-57.
14. van de Ven C, Boeree A, Stalpers F, Zwaan CM, Den Boer ML. Ibrutinib is not an effective drug in primografts of TCF3-PBX1. Transl Oncol. 2020;13(10):100817.
15. Meissner F, Geddes-McAlister J, Mann M, Bantscheff M. The emerging role of mass spectrometry-based proteomics in drug discovery. Nat Rev Drug Discov. 2022;21(9):637-654.